ELSEVIER

Physica D 106 (1997) 49–56

PHYSICA D

Recognizing randomness in a time series

Jianbo Gao

Department of Atmospheric Sciences, University of California, Los Angeles, CA 90095-1565, USA

Received 8 July 1996; revised 22 October 1996; accepted 10 December 1996
Communicated by A.M. Albano

Abstract

We study the effects of intrinsic noise on low-dimensional chaotic systems and nonlinear oscillating systems. For the former, we show that adding increasing amounts of intrinsic noise increasingly destroys the characteristic short-term predictability of chaos, while for the latter, we show that phase points near the deterministic limit cycle execute Brownian-like motions. Quantitative methods are also proposed to estimate the amount of noise contained in the signal.

1. Introduction

Complex time series are ubiquitous. Analysis of data aims ultimately at understanding the mechanism of the underlying dynamics, so that the system under study can be modeled, predicted, and controlled. An important step which may give us an insight into the origin of the complexities observed is to answer whether the complexity is due to deterministic chaos, external noise or a combination of the two. This issue has been under extensive study recently, and several methods of detecting the deterministic structure in a data set have been proposed [1–5]. Attention has also been called to situations where noise can mimic chaos in a more subtle way [6,7] than $1/f$-like noise [8–10].

Very recently Cellucci et al. [11] have asked a practically more important question as to what extent a signal is noise corrupted. Based on Gao and Zheng embedding method [12], they have proposed an interesting algorithm for estimating the amount of additive noise contained in the signal.

Intrinsic noise is, however, equally abundant as additive noise in nature and in man-made systems. Though it is thought that detecting intrinsic noise in a signal is considerably more difficult than detecting additive noise, we should still ask questions such as what kind of rich dynamical behavior can an intrinsic noise induce? How strong is the noise level? How much can simple data analysis achieve?

In this paper we study by time series analysis the effects of intrinsic noise on two important classes of dynamical systems: low-dimensional chaotic systems and nonlinear oscillating systems. For the former, we shall show that adding increasing amount of intrinsic noise increasingly destroys the characteristic short-term predictability of chaos. This property is used to design a method to quantitatively measure the strength of the intrinsic noise. For stochastically driven nonlinear oscillators, we shall show that phase points near the deterministic limit cycle execute Brownian-like motions when the random force is not very strong. The amount of intrinsic noise can be measured by estimating the width of the diffused limit cycle.

PII S0167-2789(97)00024-9

The remaining part of the paper is organized as follows. In Section 2, we review the concept of time dependent exponent $\Lambda(k)$ curves defined in [5,12]. We then define logarithmic displacement curves to demonstrate the characteristic short-term predictability of chaos. In Section 3, we study the Lorenz system with intrinsic noise, and in Section 4, we study the stochastically driven Van de Pol's oscillator, together with an application to the analysis of a fluctuating velocity signal measured at a fixed point in the near wake of a cylinder.

2. Logarithmic displacement curves

Given a scalar time series $\{x(i),\ i = 1, \ldots, N\}$ (with sampling time δt), it is now common practice in nonlinear time series analysis to first construct vectors of the form $X_i = (x(i), x(i+L), \ldots, x(i+(m-1)L)$, with m the embedding dimension and L the delay time [13]. This defines a dynamics $F: X_i \to X_{i+1}$. An important issue for chaotic time series analysis is to determine the parameters m and L properly so that some measure of the signal is optimized.

It is demonstrated in [5,12] that chaotic time series can be conveniently studied by calculating the following time dependent exponent $\Lambda(k)$ curves:

$$\Lambda(k, m, L) = \langle \ln(\|X_{i+k} - X_{j+k}\| / \|X_i - X_j\|) \rangle \quad (1)$$

with $r \le \|X_i - X_j\| \le r + \Delta r$, where r and Δr are prescribed small distances. Geometrically $(r, r + \Delta r)$ defines a shell. The angle brackets denote ensemble averages of all possible pairs of (X_i, X_j). The integer k corresponds to the evolution time $k\delta t$. For simplicity, we call k the evolution time. With k fixed to be small, based on continuity and false nearest neighbours argument, an optimal embedding procedure can be obtained [12]. Based on this embedding procedure, Cellucci et al. [11] have developed an interesting algorithm to quantitatively measure the amount of additive noise mixed in a low-dimensional chaotic signal. After m and L are thus properly chosen, $\Lambda(k)$ increases linearly with k till some k_{p}, then flattens. We will show later that $T_{\mathrm{p}} = k_{\mathrm{p}}\delta t$ is the predictable time scale for chaos. When calculating $\Lambda(k)$ curves, the additional condition $|i - j| > w$, with w some integer, is recommended to remove the autocorrelation between points [5,12] (in this study, w is arbitrarily chosen to be 1000). By calculating $\Lambda(k)$ on a series of shells, $r_{n+1} \le \|X_i - X_j\| \le r_n,\ n = 1, 2, 3, \ldots$, we obtain a series of $\Lambda(k)$ curves. Fig. 1 shows the result for the chaotic Lorenz system (see the equations for the Lorenz system in Section 3). We see that the linear increasing part of these curves collapse nicely to form an envelope. The slope of the envelope estimates the largest positive Lyapunov exponent. The existence of this envelope in low-dimensional chaotic systems provides an effective method to distinguish chaos from noise [5].

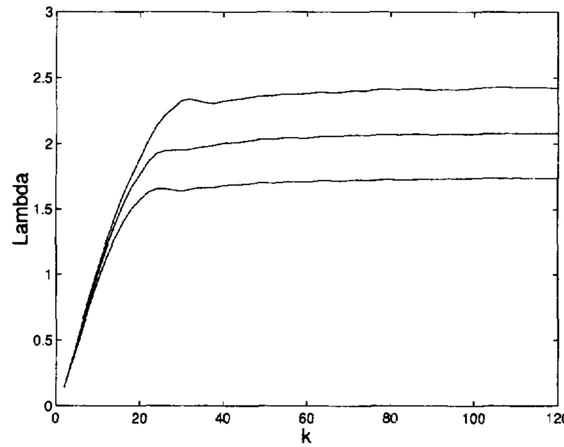

Fig. 1. $\Lambda(k)$ vs. k curves for the Lorenz system. The time series (with sampling time $\delta t = 0.06$) was first normalized to the unit interval [0, 1], then 6000 points were embedded with $m = 8$, $L = 2$. Three curves correspond to shells $(2^{-(i+1)/2}, 2^{-i/2})$ with $i = 5, 6, 7$ (these curves are the same as in [12]).

We now show that $T_{\mathrm{p}} = k_{\mathrm{p}}\delta t$ corresponds to the predictable time scale of chaos. We rewrite Eq. (1) to define the following logarithmic displacement curves:

$$\langle \ln \|X_{i+k} - X_{j+k}\| \rangle = \langle \ln \|X_i - X_j\| \rangle + \Lambda(k), \quad (2)$$

and plot $\langle \ln \|X_{i+k} - X_{j+k}\| \rangle$ vs. evolution time k. As our shells are very thin, we simply estimate $\langle \ln \|X_i - X_j\| \rangle$ as the logarithm of the outer radius of the shell. Fig. 2 shows the result for the Lorenz system. We see that for large k where $\Lambda(k)$ is constant, the curves collapse nicely. This is because all $\langle \ln \|X_{i+k} - X_{j+k}\| \rangle$

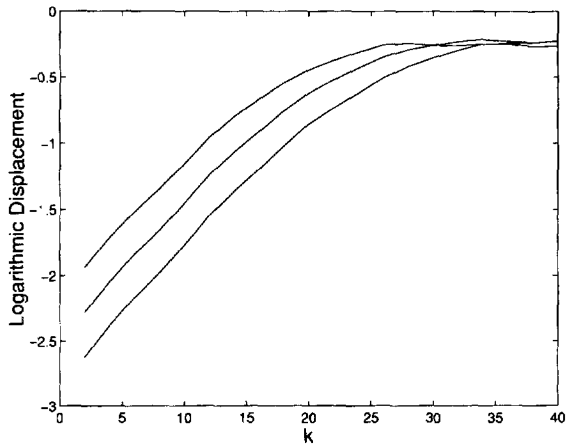

Fig. 2. The logarithmic displacement curves corresponding to Fig. 1.

are estimating the same quantity, the logarithm of the diameter of the attractor. For small k where $\Lambda(k)$ coincides to form a linear envelope, we see the displacement curves separate. Thus, within time period T_p, the pairs (X_i, X_j) on an average are keeping memory as which shell they are originating from. This is a nice demonstration of the short-term predictability of chaos.

Since noisy signals are infinitely dimensional, issues such as optimal embedding, which are pertinent to the analysis of low-dimensional chaotic signals, are not really defined in the noisy signal analysis. Therefore, in the actual computation we choose rather arbitrarily the embedding dimension m to be between 6 and 10. After m is chosen, the delay L is determined by requiring that the displacement curves (or $\Lambda(k)$ curves) be fairly smooth.

3. Stochastically driven Lorenz system

Several well-known model chaotic systems with intrinsic noise have been studied, such as the Logistic map, Henon map, Lorenz equations and Rossler equations. We choose the forced chaotic Lorenz system as an example to show some typical results.

We study the following system:

$$\mathrm{d}x/\mathrm{d}t = 10(y - x) + D\xi_1(t),$$
$$\mathrm{d}y/\mathrm{d}t = x(45.92 - z) - y + D\xi_2(t), \quad (3)$$
$$\mathrm{d}z/\mathrm{d}t = xy - 8z/3 + D\xi_3(t)$$

with $\langle \xi_i(t) \rangle = 0$, $\langle \xi_i(t)\xi_j(t\prime) \rangle = \delta_{ij}\delta(t - t')$, $i, j = 1, 2$ and 3. We note that D^2 is the variance of the Gaussian noise terms, $D\xi_i(t)$, $i = 1, 2$ and 3. If $D = 0$, Eq. (4) describes the clean Lorenz chaotic system.

We first define the strength of the intrinsic noise. Recall that the signal to noise ratio (SNR) in decibels for additive noise is defined as 10 times the base 10 logarithm of the signal variance divided by the noise variance. By interpreting the signal variance as the variance of the dynamical signal (with intrinsic noise) and noise variance as the intrinsic noise variance, we naturally have an SNR definition for intrinsic noise. We find that the variance of the signal with intrinsic noise is very close to that of the clean signal. Thus, we can simply use the variance of the clean signal to define SNR. Fig. 3 shows the logarithmic displacement curves for the forced Lorenz system with SNR = 10 and 0. Comparing Figs. 3 and 2 we notice that the separation between the linear increasing part of the curves shrinks by adding intrinsic noise: the stronger the noise is added, the more the separation shrinks.

How do we understand this feature? We better answer this in terms of the $\Lambda(k)$ curves. When there is no noise, the $\Lambda(k)$ curves coincide to form a linear envelope for small k. Thus when the $\Lambda(k)$ curves are transformed to the displacement curves, the displacement curves separate for small k. When there is intrinsic noise, the system is no longer low dimensionally chaotic, hence, the $\Lambda(k)$ curves for small k no longer coincide. This separation between the $\Lambda(k)$ curves for small k increases with increasing noise. Because of this separation in the $\Lambda(k)$ curves, the separation between the displacement curves shrinks.

Since the separation for the system without noise corresponds to the short-term predictability of chaos, we may say that adding increasing amount of intrinsic noise increasingly destroys the short-term predictability of the system. Now an important question is how to quantitatively describe this losing of predictability? First we arbitrarily choose two logarithmic displacement curves, D_1 and D_2. Then we estimate the distance between the linear increasing part of D_1

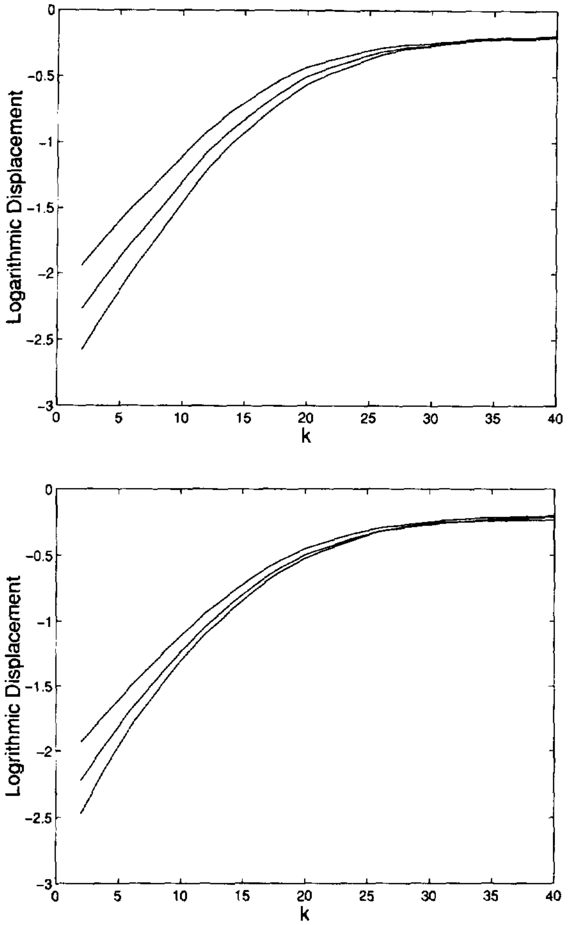

Fig. 3. The logarithmic displacement curves for the Lorenz system with intrinsic noise: (a) SNR = 10; (b) SNR = 0.

and D_2, and normalize it by the distance where there is no intrinsic noise. An alternative way is to estimate the area between D_1 and D_2, and normalize it by the area when there is no intrinsic noise. Denote the normalized distance and area by ND and NA. It is easy to see that ND and NA should be very close in magnitude. NA is, however, easier to estimate by the following approximation:

$$\mathrm{NA} \approx \frac{\sum_i (D_1(k_i) - D_2(k_i))|_{\text{with noise}}}{\sum_i (D_1(k_i) - D_2(k_i))|_{\text{without noise}}} \tag{4}$$

and

$$k_i > (m-1)L \quad i = 1, 2, 3, \ldots \tag{5}$$

Condition (5) is added to remove the dipping phenomenon in the $A(k)$ curves due to noise discovered by Cellucci et al. [11], and the correlation caused by embedding procedure such as when $k_i < (m-1)L$, $A(k)$ increases for white noise [5].

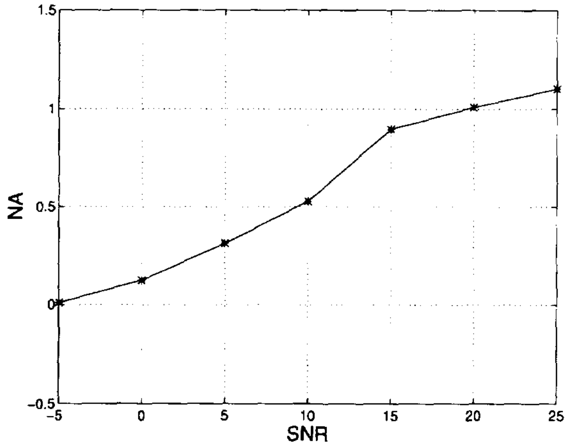

Fig. 4. NA vs. SNR curves for the Lorenz system with noise.

It is easy to see that NA = 1 when the noise is absent, and NA = 0 when the noise is sufficiently strong. We expect NA decreases monotonically with increasing noise. This is indeed the case, as shown in Fig. 4. This curve, especially the monotonic decreasing part, essentially remains unchanged when different displacement curves are chosen to calculate NA.

Before going on, we should comment on why NA > 1 for very weak noise. In designing Eq. (5), we basically assume the displacement curves collapse perfectly. However, sometimes there is deviation from this assumption. Though the deviation is small, since the area between the curves D_1 and D_2 for clean signal is not very large, this effect is not negligible. This same phenomenon sometimes causes NA > 0 instead of NA = 0 when noise is sufficiently strong. But since the profile of the curve is well defined, we consider Eqs. (4) and (5) to be reasonably good.

4. Stochastically driven Van de Pol's oscillator

Three stochastically driven nonlinear oscillators have been studied: Van de Pol's oscillator, Rayleigh's oscillator, and an oscillator generated by a force

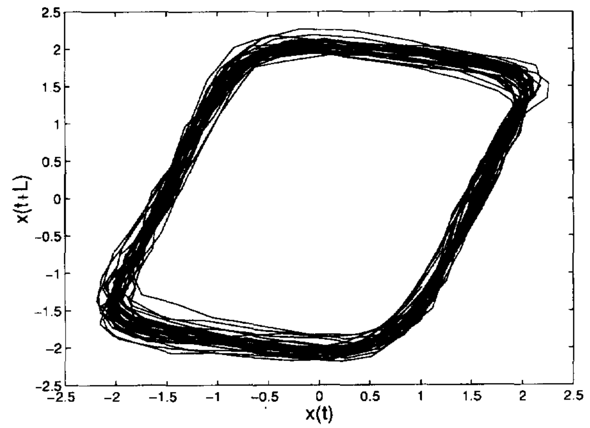

Fig. 5. A 2-D phase diagram for the stochastically forced Van de Pol's oscillator ($L = 6$, $\delta t = 0.2$).

composed of a gradient part and a circulation part [14]. We choose the first to present some typical results.

We study the following system:

$$\mathrm{d}x/\mathrm{d}t = y + D_1\xi_1(t),$$
$$\mathrm{d}y/\mathrm{d}t = -(x^2-1)y - x + D_2\xi_2(t) \tag{6}$$

with $\langle\xi_i(t)\rangle = 0$, $\langle\xi_i(t)\xi_j(t')\rangle = \delta_{ij}\delta(t-t')$, $i,j = 1,2$. Thus $D_i^2, i = 1,2$ are the variance of the Gaussian noise terms. When $D_i = 0, i = 1,2$ the system exhibits an attracting limit cycle. In this study, two situations are examined: (i) $D_1 = 0$, change D_2; (ii) $D_1 = D_2 = D$. The results are similar. The following results are based on case (ii) with sampling frequency 5 Hz.

Fig. 5 shows the phase diagram for $D = 0.1$ (SNR $= 23$). We see that limit cycle is diffused and attains some width due to stochastic force. Time series with similar phase diagrams frequently appear in diverse dynamical systems, for example, in chemical reactions [15], in fluid dynamical systems such as wakes behind a cylinder [16] and parametrically forced surface waves [17], and in plasma physics [18].

Fig. 6 shows the logarithmic displacement curves. We see that the displacement curves collapse nicely to form a single curve, which increases with k very closely as $\ln t^{1/2}$ when t is large. This feature clearly distinguishes the present system from clean or noisy

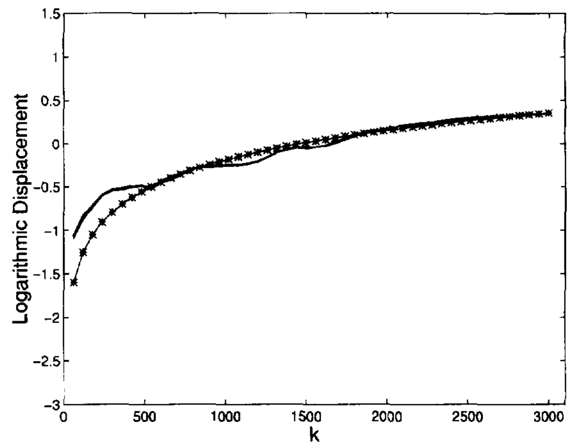

Fig. 6. The logarithmic displacement curves for the forced Van de Pol's oscillator (SNR $= 23$). The time series was first normalized to the unit interval $[0, 1]$, then 5000 points were embedded with $m = 8$, $L = 2$. Three curves correspond to shells $(2^{-(i+1)/2}, 2^{-i/2})$ with $i = 5, 6, 7$. The star curve was generated from the function $\ln t^{1/2} - 1.8$.

chaotic Lorenz system (Figs. 2 and 3). How do we understand this?

We say that this is due to the fact that the phase points execute Brownian-like motions around the deterministic limit cycle. Standard Brownian motion is characterized by the following Langevin's equation:

$$\mathrm{d}\boldsymbol{X}^2/\mathrm{d}t^2 = -f\,\mathrm{d}\boldsymbol{X}/\mathrm{d}t + \boldsymbol{F}(t)_{\mathrm{ext}}, \tag{7}$$

where $\boldsymbol{X} = (x, y, z)$ denotes the displacement vector of a particle with unit mass. The influence of the surrounding medium is split into two parts, the macroscopic dynamical friction $-f\,\mathrm{d}\boldsymbol{X}/\mathrm{d}t$ and a random force $\boldsymbol{F}(t)_{\mathrm{ext}}$. It is assumed that $\boldsymbol{F}(t)_{\mathrm{ext}}$ is independent of the position and the velocity of the moving particle. A famous result is that $\langle\boldsymbol{X}\cdot\boldsymbol{X}\rangle$, as well as $\langle x^2\rangle$, $\langle y^2\rangle$, and $\langle z^2\rangle$ (where $\langle\ \rangle$ denotes ensemble average), increases linearly with t when t is sufficiently large. This is to say, the distance between the particle and the origin grows as $t^{1/2}$ on an average. If two independent particles simultaneously wander away from the origin, the distances between them should also go as $t^{1/2}$ on an average. If we take a component of the displacement vector and embed it in a high-dimensional phase space, the distances between phase points should also vary with t as $t^{1/2}$ when t is sufficiently large. In the

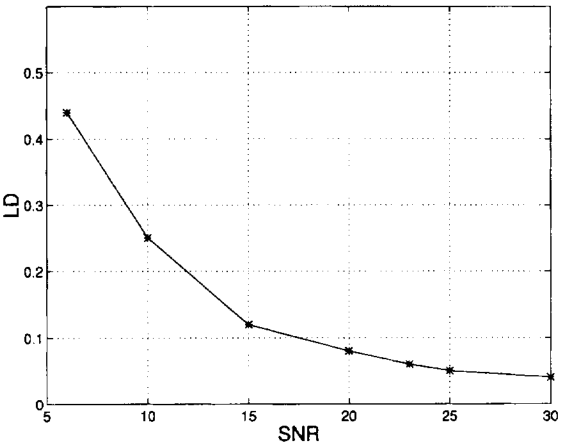

Fig. 7. LD vs. SNR curve for the forced Van de Pol's oscillator.

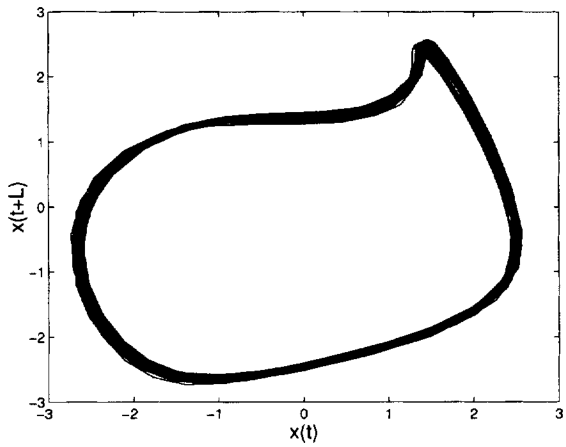

Fig. 8. A 2-D phase diagram for the measured velocity signal ($L = 6$).

case of Van de Pol's oscillator, the frictional force takes the form of $(x^2 - 1)\,\mathrm{d}x/\mathrm{d}t$. The coefficient $x^2 - 1$ is not constant now, but its average, $\langle x^2 - 1 \rangle$, is well defined. As $\langle x^2 \rangle$ measures roughly the square of the scale of the limit cycle, if the standard deviation of x^2 (which roughly measures the width of the cycle), is small compared with its mean, we may expect $x^2 - 1$ behaves on an average very much like a constant coefficient near the deterministic limit cycle. This is the underlying mechanism that our logarithmic displacement curves grow very closely as $\ln t^{1/2}$ when t is sufficiently large.

The above argument points out that if the random force driving the oscillator is so strong that particles can be kicked far off the limit cycle, a simple calculation of the logarithmic displacement curves by Eq. (3) will not enable one to get curves which grow as $\ln t^{1/2}$. Fortunately, in deliberately designed experiments to study nonlinear phenomena, situations with very strong intrinsic noise are likely to be unrealistic.

What about the case when the random force is very weak? In the limit that there is no random force, the motion is purely oscillatory, $\Lambda(k) = 0$. Hence, displacement curves are simply separated parallel constant value curves with their values equal to the logarithm of the radii of the shells. Thus, one can expect that if the random force is very weak, one will not be able to get $\ln t^{1/2}$-like curves if one does not choose shells deliberately when using Eqs. (3). Only those curves corresponding to shells with their radii smaller than the width of the cycle will follow $\ln t^{1/2}$.

The above discussion signifies the importance of estimating quantitatively the strength of the intrinsic noise. This can be done fairly easily. Based on the two geometrical scales in the system, the width and diameter of the underlying deterministic limit cycle, one can form a nondimensional number by taking their ratio. We denote it by LD. Since it is dimensionless, we expect it will only weakly depend on the embedding dimension. Hence we simply estimate it in a 2-D embedding space. For further simplicity, we isolate a small portion of the cycle, $\{x(t) : x(t) > 0,\ |x(t + L)| < \varepsilon\}$, where ε is a small number. From this sub-data set, we calculate the mean and standard deviation. A good estimation of LD is by the ratio of the standard deviation and the mean. Fig. 7 shows the result. Note that when SNR < 10, the cycle is so diffused that its shape is barely recognizable. Brownian-like motions cannot be demonstrated either.

As an application, let us study the fluctuating velocity signals measured at a fixed point in the near wake behind a circular cylinder with sampling frequency 300 Hz. The experiment was carried out in a water tunnel with very low turbulence level ($\sim 0.2\%$) with the hope that chaotic motion may be identified in the near wake. Conventional analysis of the data (such as phase diagrams, power spectra, dimension calculation,

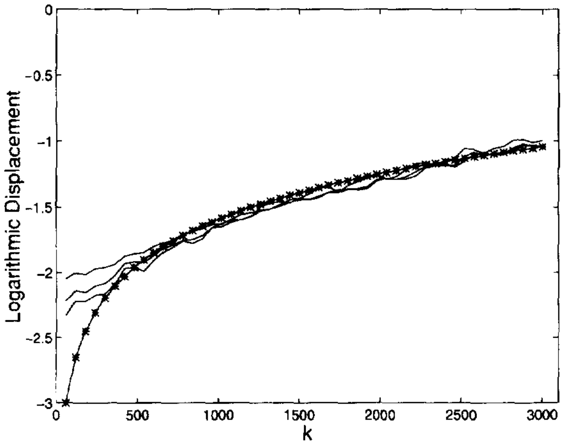

Fig. 9. The logarithmic displacement curves for the experimentally measured velocity signal. The time series was first normalized to the unit interval [0, 1], then 5000 points were embedded with $m = 8$, $L = 2$. Three curves correspond to shells $(2^{-(i+1)/2}, 2^{-i/2})$ with $i = 5, 6, 7$. The star curve was generated from the function $\ln t^{1/2} - 2.9$.

etc.) suggested that the signal exhibited chaotic feature [19].

We analyze the signal with $R_e = 136$. Fig. 8 shows the phase diagram of the signal. The logarithmic displacement curves are in Fig. 9. These $\ln t^{1/2}$-like curves clearly suggest that at least near $R_e = 136$, the signal is not generated by a chaotic motion, rather, it is generated by a nonlinear oscillator with a weak random force. It is worthy to note at this point that wakes behind a cylinder are generally regarded as a self-sustained nonlinear oscillator [20].

5. Summary and conclusion

We have studied the effects of intrinsic noise on nonlinear oscillating systems and low-dimensional chaotic systems. For the latter, it is found that intrinsic noise destroys the characteristic short-term predictability of chaos, while for the former, it is shown that phase points near the deterministic limit cycle execute Brownian-like motions. Quantitative methods are proposed to estimate roughly the amount of noise contained in the signal.

We have also included an analysis of experimental data and found that the data are very likely generated from a nonlinear oscillating system with weak intrinsic noice. We hope this analysis will stimulate application of the method proposed here.

Acknowledgements

My thanks to Dr. Paul Rapp for providing an early copy of the manuscript [11]. I would like to acknowledge with thanks Johnny Lin and Darin Hansen for their corrections to my English.

References

[1] G. Sugihara and R.M. May, Nature 344 (1990) 311.
[2] M.B. Kennel and S. Isabelle, Phys. Rev. A 46 (1992) 3111.
[3] D.T. Kaplan and L. Glass, Phys. Rev. Lett. 68 (1992) 427; Physica D 64 (1993) 431; D.T. Kaplan, Physica D 73 (1994) 38.
[4] R. Wayland, D. Bromley, D. Pickett and A. Passamante, Phys. Rev. Lett. 70 (1993) 580.
[5] J.B. Gao and Z.M. Zheng, Europhys. Lett. 25 (7) (1994) 485; Phys. Rev. E 49 (1994) 3807.
[6] P.E. Rapp, A.M. Albano, T.I. Schmah and L.A. Farwell, Phys. Rev. E 47 (1993) 2289.
[7] P.E. Rapp, A.M. Albano, I.D. Zimmerman and M.A. Jimenez-Montano, Phys. Lett. A 192 (1994) 27.
[8] A.R. Osborne and A. Provenzale, Physica D 35 (1989) 357; A. Provenzale, A.R. Osborne and R. Soj, Physica D 47 (1991) 361.
[9] J. Theiler, Phys. Lett. A 155 (1991) 480.
[10] A. Provenzale, L.A. Smith, R. Vio and G. Murante, Physica D 58 (1992) 31.
[11] C.J. Cellucci, A.M. Albano and P.E. Rapp, Detecting noise in a time series (1996), to be published.
[12] J.B. Gao and Z.M. Zheng, Phys. Lett. A 181 (1993) 153.
[13] N.H. Packard, J.P. Crutchfield, J.D. Farmer and R.S. Shaw, Phys. Rev. Lett. 45 (1990) 712; F. Takens, in: Dynamical Systems and Turbulence, eds. D.A. Rand and L.S. Young, Lecture Notes in Mathematics, Vol. 898 (Springer, Berlin, 1981) p. 366.
[14] G. Hu, T. Ditzinger, C.Z. Ning and H. Haken, Phys. Rev. Lett. 71 (1993) 807.
[15] X.G. Wu and R. Kapral, Phys. Rev. Lett. 70 (1993) 1940.
[16] K.R. Sreenivasan, in: Frontiers in Fluid Mechanics, eds. S.H. Davis and J.L. Lumley (Springer, Berlin, 1985) p. 41; C.W. Van Atta and M. Gharib, J. Fluid Mech. 174 (1987) 113; G.E. Karniadakis and G.S. Triantafylow, J. Fluid Mech. 199 (1989) 441.

[17] S. Ciliberto and J. Gollub, J. Fluid Mech. 158 (1985) 381.
[18] S.A. Stafford, M. Kot and J.R. Roth, J. Appl. Phys. 68 (1990) 488.
[19] Z.B. Lin, X.Q. Er and J.B. Gao, Sci. in China (Ser. A) 23 (1993) 277 (in Chinese).
[20] E. Berger and R. Wille, Ann. Rev. Fluid Mech. (1972) 1442; K.R. Sreenivasan, in: Whither Turbulence? Turbulence at Crossroads, ed. J.L. Lumley (Springer, Berlin, 1989) p. 269.